

Higher moments of multiplicity fluctuations in a hadron-resonance gas with exact conservation laws

Jing-Hua Fu*

Institute of Particle Physics, Central China Normal University, Wuhan 430079, PR China

Key Laboratory of Quark & Lepton Physics (CCNU), Ministry of Education, PR China

(Dated: January 27, 2023)

Higher moments of multiplicity fluctuations of hadrons produced in central nucleus-nucleus collisions are studied within the hadron-resonance gas model in the canonical ensemble. The conservation of three charges, baryon number, electric charge, and strangeness, is enforced in the large volume limit. Moments up to the forth order of various particles are calculated at SPS, RHIC and LHC energies. The asymptotic fluctuations within a simplified model with only one conserved charge in the canonical ensemble are discussed where simple analytical expressions for moments of multiplicity distribution can be obtained. Moments products of net-proton, net-kaon, and net-charge distributions in Au + Au collisions at RHIC energies are calculated and compared to the experimental measurements. The pseudo-rapidity coverage dependence of net-charge fluctuation is discussed.

PACS numbers: 24.10.Pa, 24.60.Ky, 25.75.-q

I. INTRODUCTION

The Beam Energy Scan (BES) program at the Relativistic Heavy-Ion Collider (RHIC) facility aims at studying in detail the QCD phase structure. Nonmonotonic behavior in the fluctuations of globally conserved quantities, such as net-baryon, net-charge, and net-strangeness numbers, as a function of beam energy are believed to be good signatures of a phase transition and a QCD critical point (CP) [1, 2].

Event-by-event distributions of conserved quantities within a limited acceptance are characterized by the moments, such as the mean (M), the standard deviation (σ), the skewness (S), and the kurtosis (κ). These moments are related to the corresponding higher-order thermodynamic susceptibilities and to the correlation length of the system, with increasing sensitivity for higher order moments [3, 4]. The products of the moments, such as σ^2/M , $S\sigma$, and $\kappa\sigma^2$, are constructed in order to cancel the volume term and allow for a direct comparison of experimental measurement and theoretical calculation.

Particle production at the time of freeze-out in heavy-ion collisions from SIS up to LHC energies exhibit thermal characteristics and are well described by the hadron-resonance gas (HRG) model [5]. Since the sensitivity to critical dynamics grows with the increasing order, the values of higher-order moments of charge fluctuations can differ significantly from the results of HRG along the freeze-out curve even if lower-order moments agree [2]. The HRG model results on moments of charge fluctuations can serve as a theoretical baseline for the analysis of heavy-ion collisions to properly assess the discriminating power of these observables.

In the applications of the HRG model in nucleus-nucleus collisions, one prefers to use the grand canonical ensemble (GCE) which is the most convenient one

from the technical point of view, and because of the fact that both the canonical ensemble (CE) and microcanonical ensemble (MCE) are equivalent to the GCE in the thermodynamic limit.

The applicability of the statistical approach formulated within various statistical ensembles has been considered for average quantities. In the GCE, chemical potentials and temperature are introduced to control the material and motional conservation on the average, which implies fluctuations around the average from event to event. The GCE can be used when the number of carriers of conserved charge is large enough and the fluctuations can be neglected [6]. The CE, where the material conservation laws are strictly obeyed, is relevant for systems with a large number of all produced particles, but a small number of carriers of conserved charges like electric charge, baryon number, strangeness or charm [7, 8]. This may happen not only in elementary $p\bar{p}$, $p\bar{p}$ and e^+e^- collisions [9], but also in pA or even AA collisions [10–12]. Finally, the MCE, where both the motional and material conservation laws are strictly fulfilled, has been used for elementary collisions at low energies where a small number of particles is produced [13].

The different statistical ensembles are not equivalent for small systems. When the system volume increases, the average quantities obtained with the GCE, CE, and MCE approach each other in the large-volume limit, $V \rightarrow \infty$, which is called the thermodynamical equivalence of the statistical ensembles. The thermodynamic equivalence, however, means only that the average quantities obtained in different ensembles are equal to each other in the thermodynamic limit, and is not applied to the scaled variance of particle number fluctuations [14, 15]. There is a qualitative difference in the properties of the mean multiplicity and the scaled variance of multiplicity distribution in statistical models. Expressed in terms of the scaled variance, the particle number fluctuations have been found to be suppressed in the CE and MCE comparing to the GCE and this suppression sur-

* fujh@mail.ccnu.edu.cn

vives in the limit $V \rightarrow \infty$, i.e., the differences preserved in the thermodynamic limit. Thus, the scaled variance is sensitive to conservation laws obeyed by a statistical system.

Most of the recent calculations [16–22] on the higher moments of multiplicity fluctuations in the HRG model employed only the GCE treatment. To approximately achieve conditions of the GCE, one is required to study fluctuations in a restricted phase space [23, 24]. This is usually fulfilled since there are cuts in rapidity and/or transverse momentum of the detected particles. The smaller the fraction of observed particles the smaller is the effect of global charge conservation. However, care has to be taken that these cuts do not destroy the underlying correlations responsible for the physics one tries to access.

Data on moments of net-proton, net-kaon and net-charge multiplicity distributions were recently obtained by the STAR and PHENIX Collaboration in Au + Au collisions at several collision energies and centralities [25–29]. Although no significant deviation from the Poisson expectation is observed within uncertainties for net-charge and net-kaon moments products, some pronounced structure is found in the energy dependence of $\kappa\sigma^2$ of net-proton distributions from the 0% – 5% most central collisions within $0.4 < p_T < 2$ GeV/c and at mid-rapidity $|y| < 0.5$ for energies below 39 GeV. The same measurement becomes close to the Poisson expectations when the p_T or rapidity acceptance decreases.

As the collision energy decreases and phase space coverage increases, a larger fraction of the total (conserved) charge is observed, and the conservation laws might have some impact on the multiplicity and charge fluctuations. The higher (third and forth) order moments of multiplicity distributions in the HRG model have not been calculated explicitly in the CE. The present work will address the higher order fluctuations in the general multispecies hadron gas including all mesons up to the $K_4^*(2045)$, baryons up to the Ω^- and carrying three additive charges, baryon number, strangeness, and electric charge, in the CE.

This paper is organized as follows: In the next section the partition function and the first four moments of multiplicity distributions in the CE are presented. The complete expression for high order moments of multiplicity distributions in the CE are complicated. To get an more direct idea about the extra-Poisson fluctuations in the CE, a simple illustrative example with only one type of conserved charge is discussed, where simple analytical expressions for moments of multiplicity distribution can be obtained. In Sec. III and IV the Monte Carlo simulation procedures and resonance decay contributions are described. In Sec. V the first four moments of net-proton, net-kaon and net-charge multiplicity distributions are calculated in the HRG model in CE with exact conservation of baryon number, electric charge and strangeness. The results are compared with the GCE

results and the experiment measurements. The pseudo-rapidity coverage dependence of net-charge fluctuation is discussed. Section VI presents the summary and conclusions.

II. MULTIPLICITY FLUCTUATIONS IN THE CANONICAL ENSEMBLE

In the HRG model the partition function contains all relevant degrees of freedom of the confined, strongly interacting matter and implicitly includes interactions that result in resonance formation. The GC partition function of a hadron-resonance gas can be written as a product of partition functions of all hadrons and resonances, following the notations of Ref. [15],

$$Z_{\text{GC}}(\{\lambda_j\}) = \prod_j \exp \left[\sum_{n_j=1}^{\infty} \frac{z_{j(n_j)} \lambda_j^{n_j}}{n_j} \right], \quad (1)$$

where

$$z_{j(n_j)} = (\mp 1)^{n_j+1} \frac{g_j V}{2\pi^2 n_j} T m_j^2 K_2 \left(\frac{n_j m_j}{T} \right), \quad (2)$$

K_2 is the modified Bessel function, λ_j is the fugacity for each particle species j , m_j is the hadron mass, $g_j = 2J_j + 1$ is the spin degeneracy, V is the volume of the hadron gas, the upper sign for fermions and the lower for bosons. Retaining just the first ($n_j = 1$) term corresponds to the classical Boltzmann approximation.

In the CE, the partition function does not factorize into one-species expressions because of the constraint of fixed charges. Consider a hadron gas with three abelian charges, i.e., baryon number B , strangeness S and electric charge Q . Denote them by a vector $\vec{Q} = (Q_1, Q_2, Q_3) = (B, S, Q)$ with components of these charges and by $\vec{q}_j = (q_{1,j}, q_{2,j}, q_{3,j}) = (b_j, s_j, q_j)$ the vector of charges of the hadron species j . The canonical partition function with charges \vec{Q} can be written as

$$Z_{\vec{Q}} = \left[\prod_{i=1}^3 \frac{1}{2\pi} \int_0^{2\pi} d\phi_i e^{-iQ_i \phi_i} \right] Z_{\text{GC}}(\{\lambda_j\}), \quad (3)$$

where Wick-rotated fugacities $\lambda_j = \exp[i \sum_i q_{i,j} \phi_i]$ are introduced in the GC partition function Z_{GC} .

The moments of multiplicity distributions of a set h of hadron species can be calculated by inserting a suitable fictitious fugacity into the function Z_{GC} , i.e., replacing λ_j with $\lambda_h \lambda_j$ in Eq. (3) if $j \in h$, and taking derivatives with respect to λ_h . The results of the first four moments are:

$$\langle N_h \rangle = \frac{1}{Z_{\vec{Q}}} \frac{\partial Z_{\vec{Q}}}{\partial \lambda_h} \Big|_{\lambda_h=1} = \sum_{j \in h} \sum_{n_j=1}^{\infty} z_{j(n_j)} \frac{Z_{\vec{Q}-n_j \vec{q}_j}}{Z_{\vec{Q}}}, \quad (4)$$

$$\begin{aligned} \langle N_h^2 \rangle &= \frac{1}{Z_{\vec{Q}}} \left[\frac{\partial}{\partial \lambda_h} \left(\lambda_h \frac{\partial Z_{\vec{Q}}}{\partial \lambda_h} \right) \right]_{\lambda_h=1} \\ &= \sum_{j \in h} \sum_{n_j=1}^{\infty} n_j z_{j(n_j)} \frac{Z_{\vec{Q}-n_j \vec{q}_j}}{Z_{\vec{Q}}} + \sum_{j \in h} \sum_{n_j=1}^{\infty} z_{j(n_j)} \sum_{k \in h} \sum_{n_k=1}^{\infty} z_{k(n_k)} \frac{Z_{\vec{Q}-n_j \vec{q}_j - n_k \vec{q}_k}}{Z_{\vec{Q}}}, \end{aligned} \quad (5)$$

$$\begin{aligned} \langle N_h^3 \rangle &= \frac{1}{Z_{\vec{Q}}} \left[\frac{\partial}{\partial \lambda_h} \left(\lambda_h \frac{\partial}{\partial \lambda_h} \left(\lambda_h \frac{\partial Z_{\vec{Q}}}{\partial \lambda_h} \right) \right) \right]_{\lambda_h=1} \\ &= \sum_{j \in h} \sum_{n_j=1}^{\infty} n_j^2 z_{j(n_j)} \frac{Z_{\vec{Q}-n_j \vec{q}_j}}{Z_{\vec{Q}}} + 3 \left[\sum_{j \in h} \sum_{n_j=1}^{\infty} n_j z_{j(n_j)} \sum_{k \in h} \sum_{n_k=1}^{\infty} z_{k(n_k)} \frac{Z_{\vec{Q}-n_j \vec{q}_j - n_k \vec{q}_k}}{Z_{\vec{Q}}} \right] \\ &\quad + \sum_{j \in h} \sum_{n_j=1}^{\infty} z_{j(n_j)} \sum_{k \in h} \sum_{n_k=1}^{\infty} z_{k(n_k)} \sum_{l \in h} \sum_{n_l=1}^{\infty} z_{l(n_l)} \frac{Z_{\vec{Q}-n_j \vec{q}_j - n_k \vec{q}_k - n_l \vec{q}_l}}{Z_{\vec{Q}}}, \end{aligned} \quad (6)$$

$$\begin{aligned} \langle N_h^4 \rangle &= \frac{1}{Z_{\vec{Q}}} \left[\frac{\partial}{\partial \lambda_h} \left(\lambda_h \frac{\partial}{\partial \lambda_h} \left(\lambda_h \frac{\partial}{\partial \lambda_h} \left(\lambda_h \frac{\partial Z_{\vec{Q}}}{\partial \lambda_h} \right) \right) \right) \right]_{\lambda_h=1} \\ &= \sum_{j \in h} \sum_{n_j=1}^{\infty} n_j^3 z_{j(n_j)} \frac{Z_{\vec{Q}-n_j \vec{q}_j}}{Z_{\vec{Q}}} + 4 \left[\sum_{j \in h} \sum_{n_j=1}^{\infty} n_j^2 z_{j(n_j)} \sum_{k \in h} \sum_{n_k=1}^{\infty} z_{k(n_k)} \frac{Z_{\vec{Q}-n_j \vec{q}_j - n_k \vec{q}_k}}{Z_{\vec{Q}}} \right] \\ &\quad + 3 \left[\sum_{j \in h} \sum_{n_j=1}^{\infty} n_j z_{j(n_j)} \sum_{k \in h} \sum_{n_k=1}^{\infty} n_k z_{k(n_k)} \frac{Z_{\vec{Q}-n_j \vec{q}_j - n_k \vec{q}_k}}{Z_{\vec{Q}}} \right] \\ &\quad + 6 \left[\sum_{j \in h} \sum_{n_j=1}^{\infty} n_j z_{j(n_j)} \sum_{k \in h} \sum_{n_k=1}^{\infty} z_{k(n_k)} \sum_{l \in h} \sum_{n_l=1}^{\infty} z_{l(n_l)} \frac{Z_{\vec{Q}-n_j \vec{q}_j - n_k \vec{q}_k - n_l \vec{q}_l}}{Z_{\vec{Q}}} \right] \\ &\quad + \left[\sum_{j \in h} \sum_{n_j=1}^{\infty} z_{j(n_j)} \sum_{k \in h} \sum_{n_k=1}^{\infty} z_{k(n_k)} \sum_{l \in h} \sum_{n_l=1}^{\infty} z_{l(n_l)} \sum_{m \in h} \sum_{n_m=1}^{\infty} z_{m(n_m)} \frac{Z_{\vec{Q}-n_j \vec{q}_j - n_k \vec{q}_k - n_l \vec{q}_l - n_m \vec{q}_m}}{Z_{\vec{Q}}} \right]. \end{aligned} \quad (7)$$

A. Asymptotic fluctuations in the canonical ensemble

We describe fluctuations by various order moments of a multiplicity distribution and the products of the moments:

$$\begin{aligned} \frac{\sigma^2}{M} &= \frac{\langle (\Delta N)^2 \rangle}{\langle N \rangle}, \quad S\sigma = \frac{\langle (\Delta N)^3 \rangle}{\langle (\Delta N)^2 \rangle}, \\ \text{and} \quad \kappa\sigma^2 &= \frac{\langle (\Delta N)^4 \rangle - 3\langle (\Delta N)^2 \rangle}{\langle (\Delta N)^2 \rangle}, \end{aligned} \quad (8)$$

where N is the multiplicity of any hadron species and $\Delta N = N - \langle N \rangle$.

To get an idea about the extra-Poisson fluctuations in the CE, a simple illustrative example was introduced in Ref. [15], by neglecting baryon number and strangeness, i.e., considering only electric charge. Also neglecting possible hadrons with two or more units of electric charge and within the classical Boltzmann approximation, the following asymptotic expression for the variance of a

hadron species j can be obtained [15]:

$$\langle (\Delta N_j)^2 \rangle = \langle N_j \rangle \left[1 - \frac{\langle N_j \rangle_{\text{GC}}}{\langle h^+ \rangle_{\text{GC}} + \langle h^- \rangle_{\text{GC}}} \right] + \mathcal{O}(V^{-1}), \quad (9)$$

where $\langle N_j \rangle_{\text{GC}}$, $\langle h^+ \rangle_{\text{GC}}$ and $\langle h^- \rangle_{\text{GC}}$ are the mean multiplicities of hadron species j , positive and negative hadrons respectively in the GC ensemble. Eq. (9) show that, in the thermodynamic limit $V \rightarrow \infty$, the deviation from the Poisson statistics, $\langle (\Delta N_j)^2 \rangle = \langle N_j \rangle$, is proportional to the relative weight, in terms of multiplicity of the species j with respect to all species carrying a non-vanishing value of the same charge, $\frac{\langle N_j \rangle_{\text{GC}}}{\langle h^+ \rangle_{\text{GC}} + \langle h^- \rangle_{\text{GC}}}$. This nicely meets our physical intuition that, in a system with many species, the distribution of single and rarely produced ones is little affected by global conservation laws. Conversely, the scaled variance of the most inclusive sets are strongly affected by the conservation laws and can show large deviations from Poisson statistics.

Following the same derivation as Ref. [15], within this simple model and the Boltzmann approximation, we ob-

tain for the third and forth order cumulants:

$$\langle(\Delta N_j)^3\rangle = \langle N_j \rangle \left[1 - 3 \frac{\langle N_j \rangle_{\text{GC}}}{\langle h^+ \rangle_{\text{GC}} + \langle h^- \rangle_{\text{GC}}} \right] + \mathcal{O}(V^{-1}) \quad (10)$$

and

$$\begin{aligned} \langle(\Delta N_j)^4\rangle - 3\langle(\Delta N_j)^2\rangle \\ = \langle N_j \rangle \left[1 - 7 \frac{\langle N_j \rangle_{\text{GC}}}{\langle h^+ \rangle_{\text{GC}} + \langle h^- \rangle_{\text{GC}}} \right] + \mathcal{O}(V^{-1}). \end{aligned} \quad (11)$$

From Eqs. (10) and (11), for the higher order cumulants, the deviation from the Poisson statistics is proportional to the same relative multiplicity weight as the second order, but with a larger coefficient, which indicates a larger canonical suppression of the higher order fluctuation. Likewise, for the cumulants of the set of all positive and negative hadrons similar relations hold, only modifying N_j to all positive and negative multiplicities respectively.

To test whether the expressions from the simplified model, Eqs. (9) - (11), are valid in the full hadron gas, moment products, σ^2/M , $S\sigma$, and $\kappa\sigma^2$, of different sets of primary hadrons, π^+ , π^- , K^+ , K^- , p , \bar{p} , positive (N_+) and negative (N_-) charged particles, are calculated in the CE HRG model at SPS, RHIC and LHC energies, and the results are presented in Fig. 1 (left). The results are obtained with an extended version of the thermal model program THERMUS, as explained in detail in the following Sec. III. The dashed lines indicate the Poisson expectation. The right part of Fig. 1 presents multiplicities of π^+ , π^- , K^+ , K^- , p , \bar{p} , positive and negative charged particles with respect to total multiplicity of all species carrying a non-vanishing value of the same charge, where N_Q indicates multiplicity of particles with a nonzero electric charge, $N_{Q,S}$ indicates multiplicity of particles with a nonzero electric charge or strangeness, and $N_{Q,B}$ a nonzero electric charge or baryon number.

From Fig. 1 we see that, qualitatively, the asymptotic relations Eqs. (9) - (11) are approximately satisfied in the full hadron gas. Generally, higher order fluctuations in the CE have larger deviation (suppression) from the Poisson expectation, and the deviation is larger where the relative density of the species under study is larger. At low energies, the moments products of proton are largely suppressed, and K^+ suppresses more than K^- . As the collision energy increases, the particle and anti-particle densities approach each other and their moments products become similar. The second order fluctuation results obtained here are in good agreement with previously reported values [14, 15]. These asymptotic relations hold better for single hadron species pion, kaon and proton. For all positive and negative charged hadrons, the third and fourth order cumulants do not seem to suppress as much as those predicted by Eqs. (10) and (11). Nevertheless, these asymptotic relations can be taken as “rules of thumb” to make estimates of the products of the moments to a first approximation.

III. FREEZE-OUT CONDITIONS IN HEAVY-ION COLLISIONS

There is a phenomenological relation between the collision energy and the corresponding thermal parameters, which defines the so called chemical freeze-out line in the temperature and baryon chemical potential plane [30]. With increasing colliding energy, the system temperature increases. This is accompanied by a drop in baryon chemical potential, which can be parameterized by the following function [30]:

$$\mu_B(\sqrt{s_{NN}}) = 1.308 \text{ GeV} / (1 + 0.273 \text{ GeV}^{-1} \sqrt{s_{NN}}), \quad (12)$$

where $\sqrt{s_{NN}}$ is the c. m. energy in units of GeV. The chemical freeze-out temperature is determined by $\langle E \rangle / \langle N \rangle \approx 1.08$ GeV [31], for energy per hadron. Other model parameters, the chemical potentials related to strangeness and isospin, are constrained by strangeness conservation and by total charge over total baryon $Q/B = 0.4$, respectively. The strangeness saturation factor γ_s has been set to 1.

For the CE calculation, the needed intensive input parameters are the temperature T and the charge densities. The temperature and baryon density ρ_B are determined from the GCE results at the same energy, and the values of T and ρ_B at different collision energies are listed in Table I. The strangeness density ρ_S is set to zero, and the electric charge density is set to $\rho_Q = 0.4\rho_B$, corresponding to the ratio Z/A of Pb + Pb and Au + Au collisions.

The simulation can be carried out only with a finite volume. The computing time of the integral of Eq. (3) increases largely as the baryon number of the system increases [32]. We choose volume $V = 1000 \text{ fm}^3$ for c. m. energy $\sqrt{s_{NN}}$ below 100 GeV and $V = 3000 \text{ fm}^3$ for c. m. energy above 100 GeV. Because of the large volume, which is used to ensure effective reaching of the thermodynamic limit [11, 15], the efficiency of these runs is very low.

An extended version of the thermal model program THERMUS [32] is used in this analysis. Quantum statistics and the finite width of resonances have been taken into account. The standard THERMUS particle table includes all mesons (up to the $K_4^*(2045)$) and baryons (up to the Ω^-) listed in the July 2002 Particle Physics Booklet [33], and their respective decay channels. Weak decays are not included in the calculations.

IV. EFFECT OF RESONANCE DECAYS

In the HRG model, after thermal “production”, resonances and heavier particles are allowed to decay, therefore contributing to the final yields of lighter mesons and baryons. The ensemble averaged final particle yields, af-

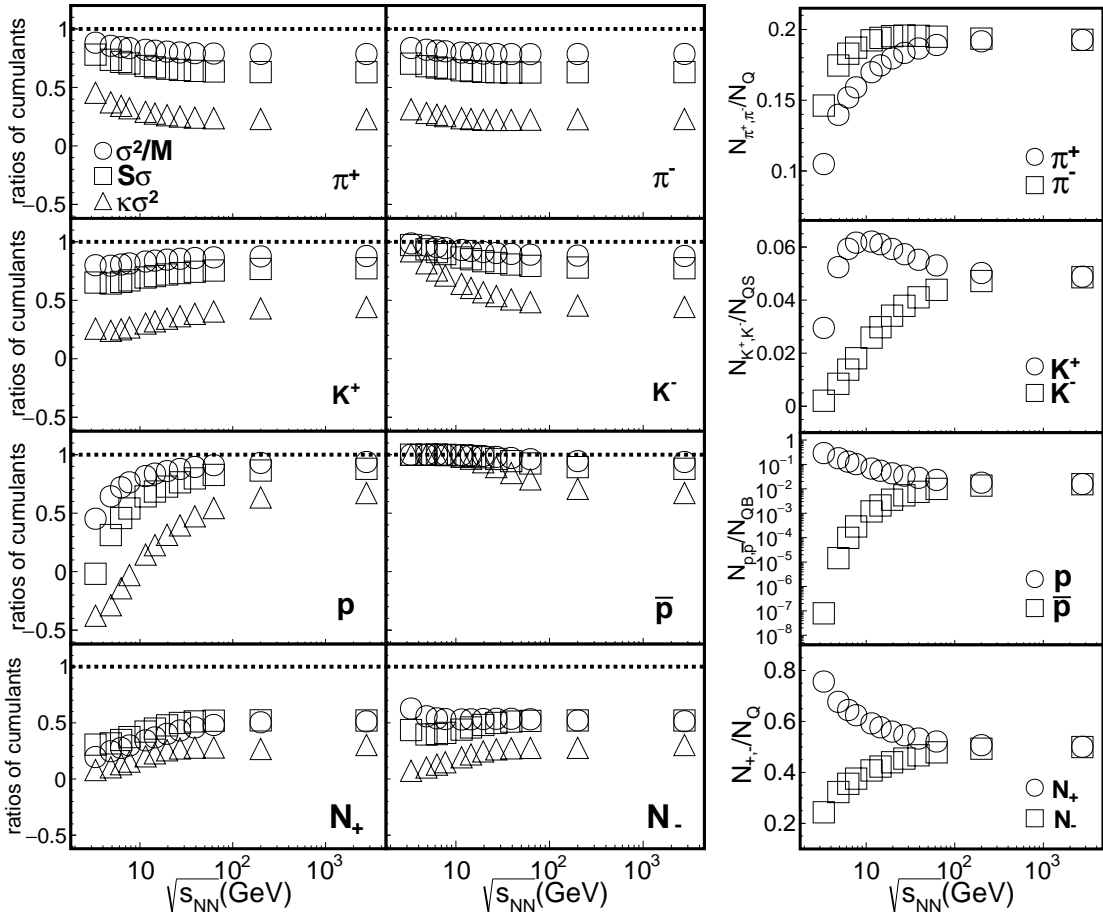


FIG. 1. (left) The products of the moments, σ^2/M , $S\sigma$, and $\kappa\sigma^2$, of different sets of primary hadrons, π^+ , π^- , K^+ , K^- , p , \bar{p} , positive (N_+) and negative (N_-) charged particles, in the CE HRG model at SPS, RHIC and LHC energies. (right) Multiplicities of π^+ , π^- , K^+ , K^- , p , \bar{p} , positive and negative charged particles with respect to total multiplicity of all species carrying a non-vanishing value of the same charge, where N_Q indicates multiplicity of particles with a nonzero electric charge, $N_{Q,S}$ a nonzero electric charge or strangeness, and $N_{Q,B}$ a nonzero electric charge or baryon number.

$\sqrt{s_{NN}}$ (GeV)	3.32	4.85	6.27	7.7	11.5	14.5
T (MeV)	94.7	117.9	129.9	137.8	149.0	153.4
ρ_B (fm ⁻³)	0.093	0.112	0.118	0.118	0.107	0.097
$\sqrt{s_{NN}}$ (GeV)	19.6	27	39	62.4	200	2760
T (MeV)	157.4	160.1	161.9	163.0	163.7	163.8
ρ_B (fm ⁻³)	0.081	0.065	0.048	0.032	0.010	0.0008

TABLE I. Temperature and baryon density at chemical freeze-out for central Au + Au (Pb + Pb) collisions at SPS, RHIC and LHC energies.

ter resonance decays, equal to [34, 35]

$$\langle N_i \rangle = \langle N_i^* \rangle + \sum_R \langle N_R \rangle \langle n_i \rangle_R, \quad (13)$$

where N_i^* and N_R denote the primordial yields of particles of species i and resonances R , the summation \sum_R runs over all types of resonances, and $\langle n_i \rangle_R \equiv \sum_r b_r^R n_{i,r}^R$

is the average over resonance decay channels. The parameter b_r^R is the branching ratio of the r -th branch of resonance R decay, and $n_{i,r}^R$ is the number of particles of species i produced in the decay of resonance R via the decay mode r .

Resonance decay has a probabilistic character. This itself causes the particle number fluctuations in the final state. The two particle correlations after resonance decays can be calculated as [34, 35]

$$\begin{aligned} \langle \Delta N_i \Delta N_j \rangle &= \langle \Delta N_i^* \Delta N_j^* \rangle + \sum_R \langle N_R \rangle \langle \Delta n_i \Delta n_j \rangle_R \\ &+ \sum_R \langle \Delta N_i^* \Delta N_R \rangle \langle n_j \rangle_R + \sum_R \langle \Delta N_j^* \Delta N_R \rangle \langle n_i \rangle_R \\ &+ \sum_{R,R'} \langle \Delta N_R \Delta N_{R'} \rangle \langle n_i \rangle_R \langle n_j \rangle_{R'}, \end{aligned} \quad (14)$$

where $\langle \Delta n_i \Delta n_j \rangle_R \equiv \sum_r b_r^R n_{i,r}^R n_{j,r}^R - \langle n_i \rangle_R \langle n_j \rangle_R$. In the CE, because of the presence of exact charge conservation

laws, all primary particles and resonances correlate with one another, while, in the GCE, only particles of the same species do correlate, and Eq. (14) reduces to

$$\begin{aligned} \langle \Delta N_i \Delta N_j \rangle &= \langle \Delta N_i^* \Delta N_j^* \rangle \\ &+ \sum_R [\langle (\Delta N_R)^2 \rangle \langle n_i \rangle_R \langle n_j \rangle_R + \langle N_R \rangle \langle \Delta n_i \Delta n_j \rangle_R] \end{aligned} \quad (15)$$

The three and four particle correlations after resonance decays can be obtained similarly from the following generating function [35]:

$$G \equiv \prod_R \left(\sum_r b_r^R \prod_i \lambda_i^{n_{i.r}^R} \right)^{N_R}, \quad (16)$$

where λ_i are auxiliary parameters that are set to one in the final formula. The full results have been presented in Appendix A of Ref. [17], and to save space not repeated here. To calculate the resonance decay contributions to kurtosis in the CE include four times nested loop over all particles and resonances, which is again fairly computing time consuming.

In recent studies [20, 21], the resonance decay contributions have been divided into an average and a probabilistic part. For example, in Eq. (15), the second term on the right hand side is called the average part, and the third term called the probabilistic part. The combination of these two parts is called the full contribution. The resonance decay contribution in the present analysis is not separated. Wherever it is mentioned, it always refers to the full contribution.

V. MOMENTS OF NET-PROTON, NET-KAON AND NET-CHARGE MULTIPLICITY DISTRIBUTIONS ON THE CHEMICAL FREEZE-OUT CURVE

The net-particle quantities, net-proton, net-kaon, and net-charge, are formed event-by-event as, $N_{p-\bar{p}} = N_p - N_{\bar{p}}$, $N_{K^+ - K^-} = N_{K^+} - N_{K^-}$, and $N_{\text{net-charge}} = N_+ - N_-$. The cumulants of net-proton multiplicity distributions can be obtained from the cumulants of proton and anti-proton multiplicity distributions and their correlations:

$$M = \langle N_{p-\bar{p}} \rangle = \langle N_p \rangle - \langle N_{\bar{p}} \rangle, \quad (17)$$

$$\begin{aligned} \sigma^2 &= \langle (\Delta N_{p-\bar{p}})^2 \rangle \\ &= \langle (\Delta N_p)^2 \rangle + \langle (\Delta N_{\bar{p}})^2 \rangle - 2 \langle \Delta N_p \Delta N_{\bar{p}} \rangle, \end{aligned} \quad (18)$$

$$\begin{aligned} \langle (\Delta N_{p-\bar{p}})^3 \rangle &= \langle (\Delta N_p)^3 \rangle - 3 \langle (\Delta N_p)^2 \langle \Delta N_{\bar{p}} \rangle \rangle \\ &+ 3 \langle (\Delta N_p) (\Delta N_{\bar{p}})^2 \rangle - \langle (\Delta N_{\bar{p}})^3 \rangle, \end{aligned} \quad (19)$$

$$\begin{aligned} &\langle (\Delta N_{p-\bar{p}})^4 \rangle - 3 \langle (\Delta N_{p-\bar{p}})^2 \rangle^2 \\ &= [\langle (\Delta N_p)^4 \rangle - 3 \langle (\Delta N_p)^2 \rangle^2] + [\langle (\Delta N_{\bar{p}})^4 \rangle - 3 \langle (\Delta N_{\bar{p}})^2 \rangle^2] \\ &- 4 [\langle (\Delta N_p)^3 \langle \Delta N_{\bar{p}} \rangle \rangle - 3 \langle (\Delta N_p)^2 \rangle \langle \Delta N_p \Delta N_{\bar{p}} \rangle] \\ &+ 6 [\langle (\Delta N_p)^2 \langle \Delta N_{\bar{p}} \rangle^2 \rangle - 2 \langle \Delta N_p \Delta N_{\bar{p}} \rangle^2 - \langle (\Delta N_p)^2 \rangle \langle (\Delta N_{\bar{p}})^2 \rangle] \\ &- 4 [\langle (\Delta N_p) (\Delta N_{\bar{p}})^3 \rangle - 3 \langle (\Delta N_{\bar{p}})^2 \rangle \langle \Delta N_p \Delta N_{\bar{p}} \rangle]. \end{aligned} \quad (20)$$

The cumulants of proton, anti-proton and their correlations in the CE can be calculated according to Eqs. (4) - (7). Formulas for cumulants in the GCE can be found in previous publications [17]. The cumulants of net-kaon and net-charge are obtained similarly from the cumulants of K^+ and K^- and the cumulants of positive and negative charged particles, respectively.

Energy dependence of the products of the moments, σ^2/M , $S\sigma/\text{Skellam}$, and $\kappa\sigma^2$, of net-proton, net-kaon, and net-charge distributions calculated in the HRG model at RHIC energies are presented in Fig. 2. The model results are presented for primordial and final state particles in both GCE and CE at $\sqrt{s_{NN}} = 7.7, 11.5, 14.5, 19.6, 27, 39, 62.4$, and 200 GeV. The relevant primordial and final state values of moments products for net-proton, net-kaon, and net-charge for various colliding energies are summarized in Tables II - VII, respectively. The STAR results for the 0% - 5% most central Au + Au collisions are shown in Fig. 2 for comparison.

$\sqrt{s_{NN}}$ (GeV)	σ^2/M		$S\sigma/\text{Skellam}$		$\kappa\sigma^2$	
	GCE	CE	GCE	CE	GCE	CE
7.7	0.995	0.764	0.984	0.533	0.952	-0.036
11.5	1.022	0.839	0.989	0.632	0.969	0.151
14.5	1.059	0.890	0.991	0.665	0.975	0.242
19.6	1.147	0.991	0.992	0.691	0.982	0.350
27	1.314	1.166	0.993	0.701	0.986	0.453
39	1.638	1.486	0.993	0.704	0.990	0.543
62.4	2.344	2.195	0.994	0.694	0.992	0.614
200	6.828	6.296	0.994	0.712	0.993	0.664

TABLE II. Primordial net-proton σ^2/M , $S\sigma/\text{Skellam}$, and $\kappa\sigma^2$ in the GCE and CE HRG model for central Au + Au (Pb + Pb) collisions.

$\sqrt{s_{NN}}$ (GeV)	σ^2/M		$S\sigma/\text{Skellam}$		$\kappa\sigma^2$	
	GCE	CE	GCE	CE	GCE	CE
7.7	1.000	0.486	0.992	0.131	0.976	-0.376
11.5	1.026	0.553	0.994	0.187	0.986	-0.223
14.5	1.063	0.600	0.994	0.215	0.990	-0.193
19.6	1.153	0.682	0.993	0.243	0.993	-0.118
27	1.323	0.817	0.992	0.264	0.995	-0.013
39	1.651	1.056	0.990	0.278	0.996	0.099
62.4	2.369	1.576	0.988	0.283	0.997	0.199
200	6.905	4.550	0.986	0.296	0.997	0.273

TABLE III. Final net-proton σ^2/M , $S\sigma/\text{Skellam}$, and $\kappa\sigma^2$ in the GCE and CE HRG model for central Au + Au (Pb + Pb) collisions.

From Fig. 2, the GCE HRG results of σ^2/M of net-proton, net-kaon, and net-charge distributions increase with collision energy consistent with the STAR measurements. As collision energy increases, the densities and variances of both particle and anti-particle increase, in the meanwhile their differences decrease. The variance

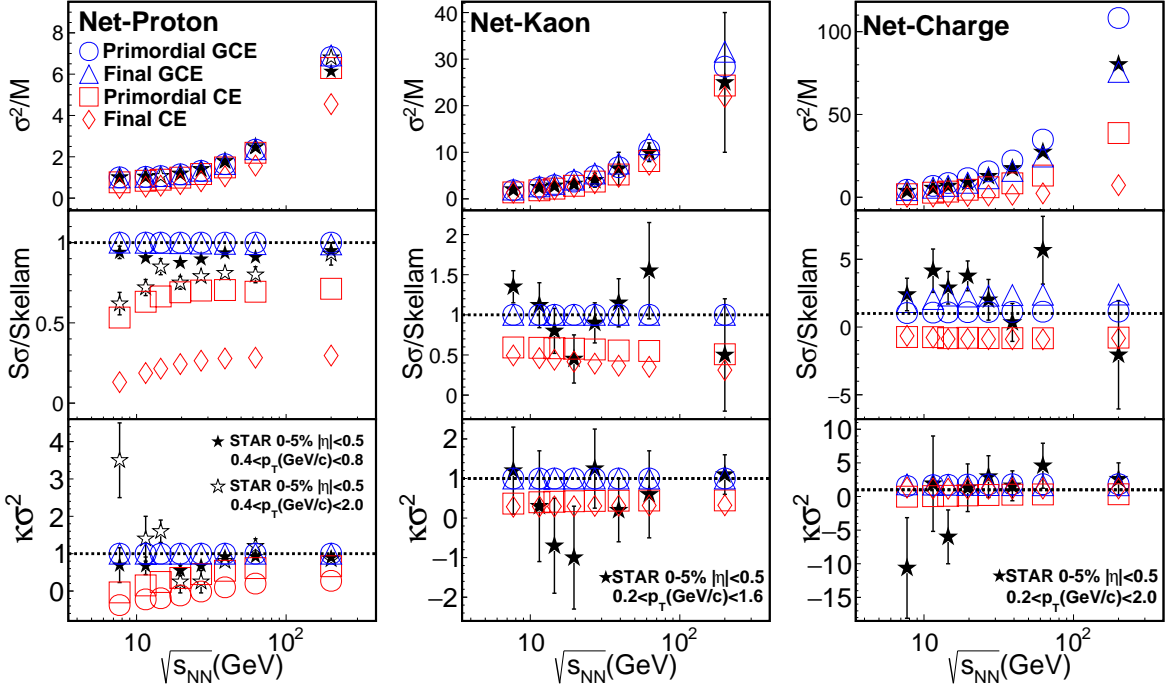


FIG. 2. Energy dependence of the products of the moments, σ^2/M , $S\sigma/\text{Skellam}$, and $\kappa\sigma^2$, for net-proton (left figure), net-kaon (middle figure), and net-charge (right figure) distributions from the HRG model and compared with the STAR data.

$\sqrt{s_{NN}}(\text{GeV})$	σ^2/M		$S\sigma/\text{Skellam}$		$\kappa\sigma^2$	
	GCE	CE	GCE	CE	GCE	CE
7.7	1.844	1.389	1.055	0.593	1.083	0.366
11.5	2.444	1.840	1.069	0.589	1.090	0.340
14.5	2.920	2.200	1.075	0.584	1.092	0.413
19.6	3.730	2.807	1.080	0.578	1.092	0.425
27	4.909	3.713	1.084	0.568	1.092	0.434
39	6.822	5.227	1.086	0.555	1.092	0.440
62.4	10.557	8.114	1.087	0.550	1.091	0.444
200	28.558	24.330	1.088	0.508	1.091	0.447

TABLE IV. Primordial net-kaon σ^2/M , $S\sigma/\text{Skellam}$, and $\kappa\sigma^2$ in the GCE and CE HRG model for central Au + Au (Pb + Pb) collisions.

$\sqrt{s_{NN}}(\text{GeV})$	σ^2/M		$S\sigma/\text{Skellam}$		$\kappa\sigma^2$	
	GCE	CE	GCE	CE	GCE	CE
7.7	2.012	1.328	1.039	0.494	1.056	0.285
11.5	2.702	1.719	1.045	0.461	1.055	0.290
14.5	3.241	2.034	1.047	0.440	1.054	0.294
19.6	4.153	2.567	1.048	0.417	1.053	0.300
27	5.474	3.372	1.049	0.392	1.051	0.307
39	7.616	4.734	1.049	0.366	1.051	0.314
62.4	11.792	7.330	1.050	0.352	1.050	0.319
200	31.794	21.891	1.050	0.311	1.050	0.323

TABLE V. Final net-kaon σ^2/M , $S\sigma/\text{Skellam}$, and $\kappa\sigma^2$ in the GCE and CE HRG model for central Au + Au (Pb + Pb) collisions.

of the net-particle is the sum of the particle and anti-particle variance, while the density of the net-particle is the difference of the particle and anti-particle density, as shown in Eqs. (17) and (18), which leads to the increase of net-particle σ^2/M with collision energy.

Since there is no resonance decays into both proton and anti-proton, the resonance decay contribution to the net-proton fluctuations in the GCE is negligible. The effect of resonance decays remains small for the net-kaon fluctuations in the GCE, but it is important for the net-charge fluctuations. Resonance decays suppress the net-charge fluctuation, σ^2/M decreasing especially at high RHIC energies. This is quite different from the total

charge fluctuation, where resonance decays increase its σ^2/M [15, 35]. Resonance decays lead to large positive correlations between positive and negative charged particles, $\langle \Delta N_+ \Delta N_- \rangle$. This term contributes positively to the total-charge variance, but negatively to the net-charge variance, c.f. Eq. (18). This essentially leads to the relative reduction of the net-charge variance when include resonance decays, and makes σ^2/M decreasing. The effect of resonance decays increases with collision energy as expected.

The net-proton and net-kaon σ^2/M from the CE HRG are mildly suppressed compared with the GCE results, while the net-charge σ^2/M from the CE HRG

$\sqrt{s_{NN}}$ (GeV)	σ^2/M		$S\sigma/\text{Skellam}$		$\kappa\sigma^2$	
	GCE	CE	GCE	CE	GCE	CE
7.7	4.526	1.836	1.031	-0.736	1.556	-0.024
11.5	6.834	2.763	1.065	-0.746	1.681	0.057
14.5	8.597	3.431	1.081	-0.782	1.729	0.106
19.6	11.514	4.531	1.098	-0.794	1.771	0.168
27	15.641	6.045	1.111	-0.813	1.798	0.226
39	22.206	8.413	1.122	-0.820	1.816	0.276
62.4	34.825	13.096	1.130	-0.828	1.827	0.311
200	108.24	38.775	1.140	-0.829	1.834	0.336

TABLE VI. Primordial net-charge σ^2/M , $S\sigma/\text{Skellam}$, and $\kappa\sigma^2$ in the GCE and CE HRG model for central Au + Au (Pb + Pb) collisions.

$\sqrt{s_{NN}}$ (GeV)	σ^2/M		$S\sigma/\text{Skellam}$		$\kappa\sigma^2$	
	GCE	CE	GCE	CE	GCE	CE
7.7	4.305	0.273	1.740	-0.651	1.806	1.325
11.5	5.737	0.454	1.853	-0.770	1.769	1.191
14.5	6.846	0.580	1.892	-0.860	1.746	1.143
19.6	8.727	0.783	1.921	-0.867	1.721	1.152
27	11.460	1.061	1.935	-0.895	1.702	1.165
39	15.904	1.500	1.939	-0.898	1.689	1.181
62.4	24.584	2.352	1.937	-0.902	1.680	1.193
200	75.705	7.299	1.928	-0.905	1.674	1.195

TABLE VII. Final net-charge σ^2/M , $S\sigma/\text{Skellam}$, and $\kappa\sigma^2$ in the GCE and CE HRG model for central Au + Au (Pb + Pb) collisions.

are strongly suppressed. The strong suppression of the net-charge σ^2/M in the CE reflects charge conservation. When resonance decays included, the final state net-charge σ^2/M from the CE HRG is approaching zero because when all the charged particles are included the net charge (Q) is exactly conserved in the CE, and there is no fluctuation.

The GCE HRG results of $S\sigma/\text{Skellam}$ and $\kappa\sigma^2$ of primordial net-proton and net-kaon are approximately one except for quantum statistical corrections. The results of net-proton are slightly suppressed by Fermi statistics, and those of net-kaon are slightly enhanced by Bose statistics. The quantum statistical corrections for net-charge is larger, because it has contributions from all stable charged particles, especially those of pion. To compare with experiment, net-charge distributions in Figs. 2 and 3 take into account only stable charged particles, while positive and negative charged particles in Fig. 1 include all primary charged hadrons. Stable charged particles here include π^+ , π^- , K^+ , K^- as well as p , Σ^+ , Σ^- , Ξ^- , Ω^- and their respective anti-baryons.

The CE HRG results of $S\sigma/\text{Skellam}$ and $\kappa\sigma^2$ of net-proton and net-kaon are suppressed compared with the GCE results. The suppression of $\kappa\sigma^2$ is larger than $S\sigma/\text{Skellam}$, consistent with our previous observations for single particle species, higher order cumulants more

suppressed in the CE. For net-proton, the canonical suppression is larger at low energies, due to the large proton density and large suppression of proton cumulants at low energies. The canonical suppression of net-kaon $S\sigma/\text{Skellam}$ and $\kappa\sigma^2$ depend weakly on the collision energy. The net-kaon $S\sigma/\text{Skellam}$ is slightly more suppressed at high RHIC energies, because the K^+ and K^- skewness become close to each other at high energies, and the net-kaon skewness decreases. The net-kaon $\kappa\sigma^2$ is more suppressed at low RHIC energies, which is mainly due to the large suppression of K^+ kurtosis at low energies. Including resonance decays further suppresses net-proton and net-kaon $S\sigma/\text{Skellam}$ and $\kappa\sigma^2$ in the CE.

The primordial and final net-charge $S\sigma/\text{Skellam}$ in the CE become negative at all RHIC energies. The net-charge skewness gets positive contribution from the N_+ skewness and negative contribution from the N_- skewness. In the CE, the skewness of N_+ becomes smaller than the skewness of N_- , because the density of N_+ is larger than the density of N_- and the higher order cumulants of N_+ are more suppressed.

The STAR measured net-proton $S\sigma/\text{Skellam}$ and $\kappa\sigma^2$ depends on the p_T or rapidity acceptance. The STAR results with $0.4 < p_T < 0.8$ GeV/c (full stars in Fig. 2 (left figure)) are better described by the GCE HRG results. The STAR results of $S\sigma/\text{Skellam}$ with larger p_T acceptance, $0.4 < p_T < 2$ GeV/c, (open stars in Fig. 2 (left figure)) are suppressed compared with the smaller p_T acceptance results, and the suppression becomes larger for decreasing collision energy. This is similar to the CE HRG results with larger suppression at low energies due to the larger suppression of proton fluctuations in the CE at low energies. The STAR experiment measured suppression of net-proton $S\sigma/\text{Skellam}$ is close to the primordial CE HRG results and less than the final CE HRG results with resonance decays. The STAR measured net-proton $\kappa\sigma^2$ with larger p_T acceptance strongly increases at low energies, which is completely different from the strongly suppressed CE HRG results. The STAR results of net-kaon and net-charge $S\sigma/\text{Skellam}$ and $\kappa\sigma^2$ have large error bars, and are in consistence with the HRG results.

A. Pseudo-rapidity coverage dependence of net-charge fluctuation

The η coverage ($\Delta\eta$) dependence of net-charge fluctuation at $\sqrt{s_{NN}} = 14.5$ GeV have been presented by the STAR Collaboration in Ref. [29]. Comparison of the STAR results with the HRG results at the same energy is shown in Fig. 3. For the smallest $\Delta\eta$ window, the STAR results are well described by the primordial GCE HRG results (full lines). When $\Delta\eta$ increases, STAR measured σ^2/M decreases and $S\sigma$ increases. The dependence of net-charge σ^2/M and $S\sigma$ on $\Delta\eta$ can be interpreted as inclusion of more resonance decay contributions. At $\Delta\eta = 1$, the most central STAR results of

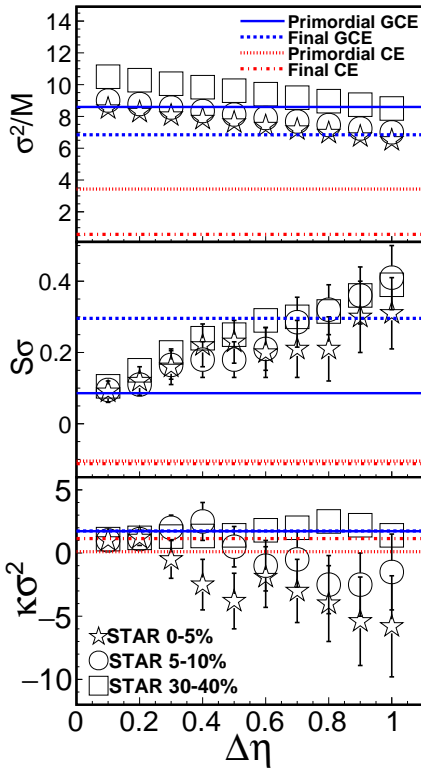


FIG. 3. Pseudo-rapidity coverage dependence of moments products, σ^2/M , $S\sigma$, and $\kappa\sigma^2$, for net-charge distributions at $\sqrt{s_{NN}} = 14.5$ GeV from the HRG model and compared with the STAR data.

σ^2/M and $S\sigma$ are well described by the final GCE HRG results (dashed lines). As explained before, resonance decays lead to large positive $\langle \Delta N_+ \Delta N_- \rangle$ and reduction of the net-charge σ^2 . This reduces σ^2/M , and increases $S\sigma = \langle (\Delta N)^3 \rangle / \sigma^2$. Notice, in Fig. 2, $S\sigma$ /Skellam is presented, while, in Figs. 1 and 3, it is simply $S\sigma$. The STAR data of $\kappa\sigma^2$ show different dependence on $\Delta\eta$ for peripheral and central collisions. Both peripheral and central STAR data points start from around $\kappa\sigma^2 = 1$ for $\Delta\eta = 0.1$. For peripheral collisions, the STAR measured $\kappa\sigma^2$ slightly increases with increasing $\Delta\eta$ to about $\kappa\sigma^2 = 2$. The GCE HRG results for both primordial and final net-charge distributions get a value of about $\kappa\sigma^2 \simeq 1.7$. For the most central collisions, the STAR measured $\kappa\sigma^2$ decreases with increasing $\Delta\eta$, but with large error bars. The CE HRG results of net-charge $\kappa\sigma^2$ are slightly lower than the GCE results.

The effects of kinematic cuts on the charge fluctuations in HRG model have been studied by several publications with mainly two kinds of approaches. In some of the studies a probability p of a single particle to be accepted is introduced [23, 36]. Others studies, instead of integrating over the entire momentum space, modify the lower and upper limits of the integral of partition function [19, 22], where the lower and upper limits are determined by the

experimental acceptance window. In the first approach, the acceptance probability p of different particle species need to be estimated. In the second approach, a modification of the single-particle spectrum to include the collective expansion might be necessary. These corrections are not implemented in the present analysis, which is still based on the original HRG model. Further studies will be carried out on how to implement the acceptance corrections consistently. From Fig. 3 we see that, at least, the tendency of the net-charge σ^2/M and $S\sigma$ versus $\Delta\eta$ can be understood nicely with the GCE plus resonance decays.

VI. CONCLUSION

Moments products up to the forth order of various particles are calculated at SPS, RHIC and LHC energies within the CE HRG model. The conservation of three charges, baryon number, electric charge, and strangeness, has been enforced in the large volume limit. The asymptotic fluctuations within a simplified model in the CE are discussed where simple analytical expressions for moments of multiplicity distribution can be obtained. Generally, higher order fluctuations in the CE have larger deviation (suppression) from the Poisson expectation, and the deviation is larger where the relative density of the species under study is larger.

The products of the moments of net-proton, net-kaon, and net-charge distributions in Au + Au collisions at RHIC energies are calculated within the HRG model in both CE and GCE and compared with the experimental measurements. The moments and their products are evaluated on the phenomenologically determined freeze-out curve in the temperature and baryon chemical potential plane. Quantum statistics and resonance decay contributions have been taken into account in the model calculations.

The GCE HRG results of σ^2/M of net-proton, net-kaon, and net-charge distributions increase with collision energy consistent with the STAR measurement. The HRG results of net-proton $S\sigma$ /Skellam in the CE are suppressed compared with the GCE results and better consistent with the STAR results with larger p_T acceptance at low energies. The STAR measured strong increase of net-proton $\kappa\sigma^2$ with larger p_T acceptance at low RHIC energies can not be understood within the GCE and CE HRG model. The net-kaon and net-charge $S\sigma$ /Skellam and $\kappa\sigma^2$ from the CE HRG are suppressed compared with those from the GCE HRG and depend weakly on the collision energy at RHIC energies.

Resonance decay contributions are important in understanding net-charge fluctuations. The STAR measured net-charge σ^2/M and $S\sigma$ dependence on pseudo-rapidity coverage can be understood as inclusion of more resonance decay contributions.

ACKNOWLEDGMENTS

The author acknowledges the support of the FANEDD of PR China under Project No. 200523 and the NNSFC under Project Nos. 10305004, 11221504.

[1] M. Asakawa, U. W. Heinz, and B. Muller, Phys. Rev. Lett. **85**, 2072 (2000).

[2] F. Karsch and K. Redlich, Phys. Lett. B **695**, 136 (2011).

[3] M. Stephanov, K. Rajagopal, and E. Shuryak, Phys. Rev. D **60**, 114028 (1999).

[4] M. A. Stephanov, Phys. Rev. Lett. **102**, 032301 (2009).

[5] A. Andronic, P. Braun-Munzinger, and J. Stachel, Nucl. Phys. A **772**, 167 (2006).

[6] P. Braun-Munzinger, K. Redlich, and J. Stachel, Particle production in heavy ion collisions, in: R. C. Hwa and X.-N. Wang (Eds.), Quark-Gluon Plasma 3, World Scientific, Singapore, 2004, pp. 491-599. e-Print: nucl-th/0304013.

[7] R. Hagedorn and K. Redlich, Z. Phys. C **27**, 541 (1985).

[8] J. Cleymans and P. Koch, Z. Phys. C **52**, 137 (1991).

[9] F. Becattini and U. Heinz, Z. Phys. C **76**, 269 (1997).

[10] J. Cleymans, K. Redlich, and E. Suhonen, Z. Phys. C **51**, 137 (1991);

[11] J. Cleymans, A. Keränen, M. Marais and E. Suhonen, Phys. Rev. C **56**, 2747 (1997).

[12] P. Braun-Munzinger, B. Friman, F. Karsch, K. Redlich, and V. Skokov, Phys. Rev. C **84**, 064911 (2011).

[13] K. Werner and J. Aichelin, Phys. Rev. C **52**, 1584 (1995).

[14] V. V. Begun, M. I. Gorenstein, and O.S. Zozulya, Phys. Rev. C **72**, 014902 (2005).

[15] F. Becattini, A. Keränen, L. Ferroni, and T. Gabbriellini, Phys. Rev. C **72**, 064904 (2005).

[16] J. H. Fu, Phys. Lett. B **679**, 209 (2009).

[17] J. H. Fu, Phys. Lett. B **722**, 144 (2013).

[18] A. Bhattacharyya, S. Das, S.K. Ghosh, R. Ray, and S. Samanta, Phys. Rev. C **90**, 034909 (2014).

[19] P. Alba, W. Alberico, R. Bellwied, M. Bluhm, V. M. Sarti, M. Nahrgang, and C. Ratti, Phys. Lett. B **738**, 305 (2014).

[20] M. Nahrgang, M. Bluhm, P. Alba, R. Bellwied, and C. Ratti, Eur. Phys. J. C **75**, 573 (2015).

[21] D. K. Mishra, P. Garg, P. K. Netrakanti, and A. K. Mohanty, Phys. Rev. C **94**, 014905 (2016).

[22] F. Karsch, K. Morita, and K. Redlich, Phys. Rev. C **93**, 034907 (2016).

[23] A. Bzdak, V. Koch, and V. Skokov, Phys. Rev. C **87**, 014901 (2013).

[24] M. Nahrgang, T. Schuster, M. Mitrovski, R. Stock, and M. Bleicher, Eur. Phys. J. C **72**, 2143 (2012).

[25] L. Adamczyk, et al., [STAR Collaboration], Phys. Rev. Lett. **112**, 032302 (2014).

[26] L. Adamczyk, et al., [STAR Collaboration], Phys. Rev. Lett. **113**, 092301 (2014).

[27] A. Adare, et al., [PHENIX Collaboration], Phys. Rev. C **93**, 011901(R) (2016).

[28] X. Luo (for the STAR Collaboration), PoS CPOD2014, 019 (2015).

[29] J. Thäder (for the STAR Collaboration), arXiv: 1601.00951.

[30] J. Cleymans, H. Oeschler, K. Redlich, and S. Wheaton, Phys. Rev. C **73**, 034905 (2006).

[31] J. Cleymans and K. Redlich, Phys. Rev. Lett. **81**, 5284 (1998).

[32] S. Wheaton, J. Cleymans, and M. Hauer, Comput. Phys. Comm. **180**, 84 (2009).

[33] K. Hagiwara *et al.*, Phys. Rev. D **66**, 010001 (2002).

[34] S. Jeon and V. Koch, Phys. Rev. Lett. **83**, 5435 (1999).

[35] V. V. Begun, M. I. Gorenstein, M. Hauer, V. P. Konchakovski, and O.S. Zozulya, Phys. Rev. C **74**, 044903 (2006).

[36] V. V. Begun, M. Gaździcki, M. I. Gorenstein, M. Hauer, V. P. Konchakovski, and B. Lungwitz, Phys. Rev. C **76**, 024902 (2007).